PCCP

Accepted Manuscript




ROYAL SOCIETY OF CHEMISTRY

www.rsc.org/pccp

# Size-Dependent Pressure-Induced Amorphization: A Thermodynamic Panorama

*Denis Machon*, Patrice Mélinon*

*Institut Lumière Matière, UMR 5306 Université Lyon 1-CNRS, Université de Lyon 69622 Villeurbanne cedex, France*

Keywords: size-effect, pressure, amorphization, thermodynamics

***Graphical Table of Contents***

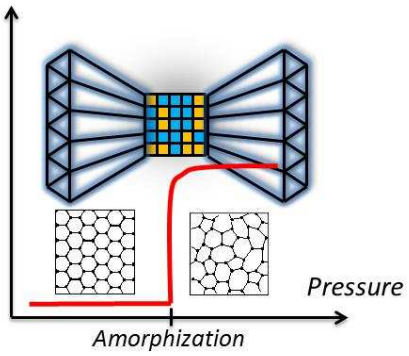


*The complex behavior of nanoparticles submitted to high-pressure is analyzed using different thermodynamic and geometrical approaches. The defect density and the surface states are identified as the main factors governing the pressure-induced transitions of nanoparticles.*

**Abstract**

Below a critical particle size, some pressurized compounds (e.g. $TiO_2$, $Y_2O_3$, PbTe) undergo a crystal-to-amorphous transformation instead of a polymorphic transition. This effect reflects the greater propensity of nanomaterials for amorphization. In this work, a panorama of thermodynamic interpretations is given: first, a descriptive analysis based on the energy landscapes concept gives a general comprehension of the balance between thermodynamics and kinetics to obtain an amorphous state. Then, a formal approach based on Gibbs energy to describe the thermodynamics and phase transitions in nanoparticles gives a basic explanation of size-dependent pressure-induced amorphization. The features of this transformation (amorphization occurs at pressures lower than the polymorphic transition pressure!) and the nanostructuration can be explained in an elaborated model based on the Ginzburg-Landau theory of phase transition and on percolation theory. It is shown that the crossover between polymorphic transition and amorphization is highly dependent on the defect density and interfacial energy, i.e., on the synthesis process. Their behavior at high pressure is a quality control test for the nanoparticles.

## 1. Introduction

To better understand the effect of surface energy on phase stability, the combination of pressure and particle size is particularly important as, keeping the particle size constant, pressure allows the energy landscapes of the system to be explored [1]. In addition, pressure and particle size are two parameters that can be used conjointly to stabilize new phases [2, 3, 4, 5]. The interest in studying nanoparticles under high-pressure is at least two-fold: (i) to gain a fundamental understanding of the thermodynamics when the interfacial energy becomes of the same magnitude as the intra-particle energy, and (ii) to stabilize new structures that may have potential interest as functional materials.

A surprising transformation favored by reducing the particle size is the crystal-to-amorphous transition [6, 7]. It is observed that amorphization in nanoparticles occurs once a critical defect density is reached. For instance, irradiated nanocrystalline $ZrO_2$ (3 nm) will amorphize whereas irradiated bulk $ZrO_2$ does not [8]. Recently, a new process for amorphizing nanoparticles has been reported: size-dependent pressure-induced amorphization. Below a critical diameter, an amorphous state is observed under pressure instead of a high-pressure polymorph. For instance, it has been shown that, below a diameter of 10 nm, $TiO_2$ nanoparticles undergo pressure-induced amorphization (PIA) whereas nano-anatase transforms to a baddeleyite structure when the diameter exceeds 10 nm [9, 10]. Such size-dependent PIA has also been reported in $Y_2O_3$ nanoparticles [11]. When the particle diameter exceeds 21 nm, the initial cubic structure exhibits a transition to a hexagonal structural phase at 14 GPa. A different scenario is observed for particles with a diameter of 16 nm, for which the cubic phase transforms to an amorphous state at 25 GPa.

A similar effect has been observed in PbTe nanoparticles [12, 13]. Below a diameter of 9 nm, PbTe nanoparticles undergo PIA whereas, with larger particles, a polymorphic transition is observed at 8 GPa.

Thermodynamic descriptions have been tentatively developed to describe this size-dependent PIA phenomenon [6, 12] but some features of the transition require a deeper understanding. One of them is the fact that amorphization occurs at a lower pressure than the expected polymorphic transformation [6, 12, 14 ]. Moreover, total amorphization is not always observed. In samples with a lower defect density, amorphization and polymorphic transformations occur simultaneously, leading to complex nanostructuration [6].

In this article, we present thermodynamic arguments that may be invoked to describe and improve our understanding of the greater propensity of nanomaterials to amorphize under pressure. In the first part, we propose a qualitative analysis based on the energy landscape concept, which is well suited as it explicitly integrates the kinetic aspect that is crucial in amorphization processes. Then, we develop a thermodynamics approach of pressure-induced phase transition, taking into account the interfacial energy. We formally derive the effects of this parameter on the transition pressure, and extend this formalism to amorphization. Finally, we determine the amorphization pressure using a geometrical approach based on percolation theory. The lowering of amorphization pressure with respect to the polymorphic transition pressure is formally derived. In the case of competition between the two mechanisms (polymorphism vs. amorphization), we use the Ginzburg-Landau theory of phase transitions by including the effects of particle size and kinetic aspects.

## 2. Description based on the energy landscapes concept

The competition between transformation into either a crystalline phase or an amorphous state is governed by a delicate balance between thermodynamic and kinetic factors. Amorphization may occur if the nucleation and growth of an equilibrium crystalline phase is kinetically hindered. To better represent this aspect, the configurational energy landscape concept is fully informative. This landscape can be depicted as a multidimensional plot of the potential energy (E) corresponding to different local and long-range arrangements of atoms in the system and

to the type of bonding [7, 15]. Each arrangement constitutes a "configuration" that is often shown schematically in two or three dimensions as a plot of E *vs.* the generalized configurational coordinates (**Figure 1**). Each crystalline polymorph in the system corresponds to a deep energy minimum. For either temperature or pressure increase, a different crystalline polymorph becomes more stable and a polymorphic transition takes place. The ease of this transition is dictated by the height of the energy barrier separating the two phases and the transformation pathway between them, involving breaking and re-forming of bonds and displacement of relative atomic coordinates. In addition to the deep and sharp energy minima representing ordered, crystalline phases, a "landscape" of amorphous states is formed by a number of shallow minima or basins of similar energies, separating the regions of stability by relatively small energy barriers. Figure 1 shows a possible energy landscape at the transition pressure between two crystalline phases 1 and 2. When the defect density in the nanoparticle is low, the energy minima of both crystalline phases are equally deep but separated by a potential energy barrier that governs the kinetics of this transition process. For a high defect density, the energy minimum of each crystalline phase is significantly increased whereas the landscape of amorphous states is only slightly affected, as amorphous states are defective and flexible structures for which relaxation processes are facilitated. At a critical defect density, the relative height of the energy barrier between phase 1 and phase 2 may exceed the critical value for the phase 1-to-amorphous transformation, resulting in a kinetically preferred crystal-amorphous transformation instead of a phase 1-to-phase 2 transformation.

In summary, two critical factors govern the amorphization process: (i) the depth of the energy minima representing different crystalline states; (ii) the height of the energy barrier with respect to the amorphous megabasin, which can be increased by the number of defects (induced by doping, irradiation, etc.), surface/interface energy, strain, etc. Whenever this increase is sufficiently high, the initial crystal structure may be destabilized in favor of a new, non-crystalline atomic configuration. Since the energy barrier between two crystalline phases

that undergo reconstructive phase transformation is higher due to bond breaking and atomic movements, amorphization may be easier to achieve.

### 3. Thermodynamics aspect derived using the Gibbs Energy

The expression of the Gibbs energy, including the interfacial energy term (γ) and considering isothermal compression, reads

$$dG = V.dP + \gamma.dA \quad (1)$$

By applying mathematical techniques of classical thermodynamics, the molar Gibbs energy including pressure and particle size (radius *r*) can be deduced and expressed as [16]

$$G_m = P.V_m + \frac{3V_m\gamma_0}{r} + G_0 \quad (2)$$

Where $\gamma_0$ is the contribution of the interfacial energy at ambient pressure.

An illustration of these considerations is given in **Figure 2**. The Gibbs energy is shown as a function of pressure. We consider a transition between a low-pressure phase (lp) and a high-pressure phase (hp) in the cases of:

i) A bulk material. The dark lines show the Gibbs energy of a low-pressure phase (lp) and a high-pressure phase (hp) in the case of a bulk sample with no size effect ($r \rightarrow \infty$). To a first approximation, the slope of the line is given by the molar volume of the phase (as $dG_m = V_m.dP$). The transition pressure is determined where the two lines cross ($G_{lp} = G_{hp}$).

ii) A nanoparticle of the same composition. Considering $\gamma_{hp} - \gamma_{lp} > 0$ as proposed by Alivisatos (where $\gamma_{hp}$ and $\gamma_{lp}$ are the surface energies of the high-pressure phase and the low-pressure phase, respectively), we predict an increase in the transition pressure for nanoparticles. This model is fully consistent with that developed by Alivisatos'

group to explain the greater transition pressure in nanoparticles than in bulk [2, 14, 17, 18].

It is important to note that in a realistic case $\gamma_0$ is variable as it corresponds to an interfacial energy term. This term should take into account not only the surface energy but the presence of defects, interactions with capping molecules and so on. For instance, this interfacial energy in nanoparticles may vary depending on the synthesis approach [14, 19]. As discussed recently [20] in the case of a nanoparticle, one has to take into account the different contributions of the surface/interface in a multidimensional plot (defect, capping molecules, etc). $\gamma_0$ results from a projection on the (G,P) plane and describes the contribution of the different nanoscale-related parameters (such as ligands, shape, size, strain constraint or confinement effect).

Therefore, $\gamma_0^{lp}$ and $\gamma_0^{hp}$ are not univocally defined and can vary from one sample to another. This may explain the discrepancies sometimes found in the literature concerning the transition pressure in nanoparticles.

For sufficiently large $\gamma_0$ and sufficiently small *r*, the free energy of the nanoparticle may be of the same order of magnitude as that of an amorphous state. **Figure 3** shows a thermodynamic picture, starting again with the same considerations above but including amorphous states. Strictly speaking, the amorphous solid does not constitute a true phase and equilibrium thermodynamic arguments should not apply. However, thermodynamic quantities such as specific volume, enthalpy, and entropy are readily measured for solid amorphous materials and can be used to describe a non-crystalline substance that is in a metastable thermodynamic equilibrium. In the case where an additional energy term related to the defective surface is included, as long as this contribution is large enough then the pressure increase may lead to the energy field of the amorphous state.

In the classical thermodynamic framework, amorphization usually results from the transformation of a superpressed crystal to an amorphous state [7] and the amorphization

pressure is higher than the polymorphic transition pressure. The introduction of a high defect density and interfacial energy can *lower* the amorphization pressure, and ultimately amorphization may occur at ambient pressure, as for irradiated nanosized $ZrO_2$ [8]. However, the approach is mainly qualitative and a formal expression of the amorphization pressure cannot be derived, contrary to theoretical developments presented in the next section.

**4. Geometrical description of amorphization: A Percolating system**

The approach based on the Gibbs energy explicitly provides the reasons for amorphization. This transition occurs when the energizing processes (defects, interfacial and elastic energies) destabilize the crystalline phase in favor of the amorphous state, i.e., when the Gibbs energy of the crystalline phase pressure exceeds that of the amorphous state. The amorphization pressure decreases when the free energy at ambient pressure is high, i.e., when the interfacial energy and the defect concentration are important. This amorphization pressure can be relatively low compared to the polymorphic transition pressure, and then the system is far from equilibrium. The difference between the amorphization pressure and the polymorphic transformation pressure is not straightforward to quantify, as the free energies of the amorphous states are not known. In the following, we propose to determine the amorphization pressure by adopting a geometrical description of the growth of the amorphous state in the framework of percolation theory. As the amorphous state becomes energetically favorable and we are far from equilibrium, growth can be considered as explosive [21]. This corresponds to the inverse phenomenon known as explosive crystallization leading to a dendritic structure. The associated kinetics being very rapid, the amorphization pressure determined by a geometrical description should be close to the one given by thermodynamic arguments. Therefore, we propose to examine the "growth"/ "propagation" of the amorphous state in a crystalline matrix in greater details in the framework of invasive percolation theory, as it has been done in the case of radiation-induced amorphization [22, 23].

Let us describe the basic assumptions of the model. A Voronoi cell can be defined around each defect. When approaching the stability field of the amorphous state, this cell can present two possible states: crystal-like or amorphous-like. This is a percolating system where we can define the "experimental" crystal-to-amorphous transition at the percolation threshold. Percolating systems have a parameter $q$ that controls the occupancy of sites (Voronoi cell) in the system. This parameter represents the probability of a site to be amorphous and increases with increasing pressure.

The Voronoi cells are independent but an amorphous cell grows during pressurization above the critical pressure. In this case, this corresponds to an invasive percolating system where the amorphous state is the invader and can penetrate an isolated crystallized region (so-called *defender*). This is called invasive percolation without trapping. It is well established that percolation without trapping and regular percolation are of the same universality class [24]. Thus, microscopic description of the transition at a local level is not necessary. The key point of the description is the fractal structure of the infinite cluster defined just above the percolation threshold. The use of a fractal dimension is dictated by the inhomogeneity of the system, contrary to homogeneous structures for which Euclidean space is adapted.

At a critical value $q=q_c$ where the percolation transition takes place, the mean cluster size given by the correlation length $\xi$ diverges following a power law

$$\xi \approx \xi_0 \left| q - q_c \right|^{-\mu} \qquad (3)$$

where $\mu$ is the critical exponent which depends on the type of percolation and the type of lattice [25].

The crystal-to-amorphous transition occurs at the percolation threshold. The offset between the pressures of polymorphic transition and of amorphization $\Delta P = P_c^* - P_c^{am}$ can be determined by [26]

$$\Delta P = \frac{\xi^{2\mu-2}}{\alpha_0 \xi^{2\mu} \Gamma^2 (3-\mu)} \quad (4)$$

where $\Gamma$ is the Euler gamma function, $\xi$ is the microscopic correlation length, and $\alpha_0$ is a numerical parameter. The maximum offset is given for an invasive percolating system $D_f$=2.5 [27] and yields

$$\Delta P_{max} \approx \frac{16\xi^{-2}}{9\alpha_0 \pi} \quad (5)$$

The microscopic correlation length $\xi$ is defined in percolation theory as the typical radius of the largest finite cluster. In the case of nanoparticles, $\xi$ cannot exceed *r*, the radius of the nanoparticle. This spatial limitation leads to

$$P_c^{am} = P_c^* - \frac{16}{9\pi\alpha_0 r^2} \quad (6)$$

where $P_c^*$ is the polymorphic transition pressure in the nanoparticle. This pressure can be expressed as (see below and Ref. [19])

$$P_C^* = P_C + 3\delta \frac{\gamma_{hp} - \gamma_{lp}}{\alpha_0 . r} \quad (7)$$

where $P_C$ corresponds to the polymorphic transition pressure in the bulk material.

Finally, $P_c^{am} = P_C + 3\delta \frac{\gamma_{hp} - \gamma_{lp}}{\alpha_0 . r} - \frac{16}{9\pi\alpha_0 r^2}$ (8)

Using these results, one can draw a schematic *pressure-size* phase diagram showing two different regimes: polymorphic transition *vs.* pressure-induced amorphization (**Figure 4**).

It has been demonstrated that amorphization occurs only when a sufficient defect density is attained in the nanoparticles [6, 14], i.e., when the number of sites is sufficient to reach the percolation threshold. For typical large nanoparticles, no amorphization is observed. In this case, the transition pressure follows a 1/r-dependence (red curve – arrow 1 in Figure 4) as determined by the classical thermodynamics approach (see previous section) or Landau theory of phase transitions [19].

When the defect density is sufficient, then amorphization may occur at a critical size (which depends on the materials: ~ 10 nm in $TiO_2$ [9, 10], ~ 9 nm and in PbTe [12, 13], ~ 16 nm in $Y_2O_3$ [11]). In that case, a crossover can occur and amorphization becomes the dominant mechanism (blue zone in Figure 4). One striking consequence is that $\Delta P > 0$, i.e., the crystal-to-amorphous transition occurs at a lower pressure than the polymorphic transformation (Figure 4 – Arrow 2 in Figure). This prediction has been observed in all experimental reports of size-dependent PIA [6, 12, 14].

It is important at this point to discuss possible experimental discrepancies depending on the analytical techniques. At the percolation threshold, the whole sample does not become amorphous ($q_c = 0.2$ for sites in the fcc lattice) [28]. However, due to the fractal nature of the amorphous state, its spatial distribution is highly inhomogeneous. The density of crystallized clusters $n$ of size $s$ ($s$ being the number of Voronoi cells) decreases rapidly according to the law $n(s) = s^{-\tau}$ ($2 < \tau < 2.5$) [28]. Consequently, the remaining crystalline domains are small (typically a few times the distance between two adjacent defects) and may be smaller than the correlation length of the characterization probe, leading to an amorphous-like material even though a significant part of the sample is still crystalline. Therefore, Raman spectroscopy or X-ray diffraction may indicate complete amorphization whereas TEM experiments will show the existence of nanoscale crystalline domains.

**5. Competition between amorphization and polymorphic transition**

In the following section, we discuss the intermediate scenario, i.e., partial amorphization (arrow 3 in figure 4). In that case, a competition between the two mechanisms (polymorphic *vs.* amorphization transitions) exists. We propose a classical Ginzburg-Landau approach to extract new insight and a better understanding of the nanostructuration.

The strength of this approach is that it is possible to describe the polymorphic transition or the amorphization with the same kind of equation. The Ginzburg-Landau theory of phase transition in nanoparticles has been developed in a recent publication [19]. Let us first summarize the formalism of this approach. The seminal work by Tolédano and Dmitriev [29] demonstrates the possibility of defining a transcendental order parameter. Thus, the Landau approach to phase transitions can be extended to study any kind of structural phase transition and an order parameter can always be determined. The Landau potential for a second order transition (the formalism can also be extended to a first order transition by using a potential of higher order) with an additional coupling term between the primary order parameter and the interfacial energies is [19]

$$F = F_0 + \alpha\eta^2 + \beta\eta^4 + \delta\eta^2.\frac{\gamma_{hp} - \gamma_{lp}}{V}S \qquad (9)$$

where S and V are the surface and volume of the nanoparticle, respectively. α changes its sign at the transition and is usually defined as $\alpha = \alpha_0(P - P_c)$. δ is the coupling constant between the primary order parameter and the surface energies. Solving the equilibrium condition equation $\frac{\partial F}{\partial \eta} = 0$ leads to equation (7).

The Landau theory of phase transitions has been extended to take into account spatial derivatives of the order-parameter that may be associated with kinetics of the transition. Such a treatment was applied to the case of type-II superconductivity [30]. Then it was used to describe the incommensurate phase [31] which shows some loss of the translational symmetry, and ultimately to describe amorphization processes [32, 33].

The master equation is given by [19]

$$F = F_0 + \alpha\eta^2 + \beta\eta^4 + \delta\eta^2.\frac{\gamma_{hp} - \gamma_{lp}}{V}S + K(\nabla\eta)^2 \qquad (10)$$

with K being the Ginzburg term related to the kinetics.

Two cases can be considered. First, spatial inhomogeneity is limited and the polymorphic transition occurs. In that case, the kinetics term (K) induced a broadening of the transition region [19]. Second, for amorphization, contrary to polymorphic transitions for which the order-parameter is associated with a single critical wave vector, the order-parameter associated with the crystal-amorphous transition varies continuously from one point to another [32].

In the description of the crystalline to amorphous transformation under irradiation [32], the Ginzburg-Landau approach was used to derive that the radius of the amorphous region is given by the following relation

$$r_N = \left(\frac{K}{\alpha_0}\right)^{1/2} (C_c - C_N)^{-1/2} + r_0 \qquad (11)$$

where $\alpha_0$ is a parameter of the Landau potential, K defines the Ginzburg term in eq. (10), and $r_0$ is the initial radius of the amorphous embryo. $C_N$ is the defect concentration at which the amorphous embryo nucleates and $Cc$ is a critical concentration at which merging of amorphous embryos occurs (i.e., the percolation threshold is reached).

It has to be noted that $r_N$ is similar to the expression of coherence length determined in percolation theory (equation (3)). The critical exponent is ½ and results from the assumption used to analytically solve the Ginzburg-Landau equation, i.e., that the system is closed to the transition conditions. In brief, this treatment is an approximation of the percolation approach detailed previously.

Therefore, two size effects can be deduced. First, as in bulk material, when $C_N$ approaches $C_c$, $r_N$ diverges and leads to amorphization. Such a concentration is explicitly dependent on several nanoparticle parameters, i.e., its size and the interfacial energy expressed as [34]

$$C_c = C_0 - \lambda \frac{\gamma}{r} \qquad (12)$$

$C_0$ is the critical concentration for bulk samples that depends on the materials and on the type of defects.

Therefore, the radius of the amorphous region is dependent on the nanoparticles' features as, combining (11) and (12)

$$r_N = \left(\frac{K}{\alpha_0}\right)^{1/2}\left[(C_0 - C_N) - \lambda\frac{\gamma}{r}\right]^{-1/2} + r_0 \qquad (13)$$

When the critical defect density is approached, amorphization is favored. Two different parameters may facilitate the amorphization process: (i) reducing the nanoparticle size. As evidenced experimentally, the smaller the nanoparticles, the greater the tendency for amorphization. (ii) increasing the interfacial energy parameter γ by varying the surface state of the nanoparticles.

Therefore, at the transition pressure, two competitive mechanisms must be considered: polymorphism *vs.* amorphization. Three cases can be considered depending on the initial defect concentration *C:*

*(i)* $C > C_c$ : the nanoparticle is entirely amorphous according to the definition of $C_c$.

(ii) $C<C_N$, no amorphous nucleates appear and only polymorphic transformation occurs (**Figure 5**, case 1).

(iii) $C_N < C < C_c$ : the final state depends on the comparison between $r_N$ and $r$. When $r_N \geq r$ , the nanoparticle becomes amorphous (Figure 5, case 2), otherwise amorphous and crystalline states coexist and the fraction of the amorphous region in the nanoparticle is given by $\left(\frac{r_N}{r}\right)^3$ (figure 5, case 3).

Considering case (iii) of coexisting crystalline and amorphous regions, kinetic factors need to be considered as well. On the one hand, the Ginzburg parameter $K$ is related to the kinetics of a polymorphic transition in nanoparticles as it widens the transition region ε ($\varepsilon \propto K^{1/2}$), as demonstrated in ZnO under pressure [19]. On the other hand, increasing $K$

leads to a larger amorphous fraction as $r_N \propto K^{1/2}$. Therefore, the kinetics factor tends to slow down the polymorphic transformation whereas it favors the amorphous state. This statement is in agreement with the general trend that amorphous states are kinetically favored states.

Figure 5 summarizes the possible processes occurring during pressurization. The polymorphic transformation occurs through a nucleation and growth mechanism (case 1 in Figures 4 and 5). The main size-dependent effect is the spreading of the transition [19].

The amorphization is related to the number of defects. It occurs suddenly at pressures lower than the polymorphic transition pressure if the percolation threshold is reached and amorphization is then complete (and explosive [21]) (Case 2 in figures 4 and 5); otherwise, amorphization is only partial (Case 3 in figures 4 and 5). In that case, the final structuration consists of a high-pressure crystalline phase co-existing with a collection of amorphous domains (case 3 in Figure 5). The contribution of each state is obtained by comparing the number of Voronoi cells corresponding to both crystal and amorphous states. We extracted this information from Raman spectroscopy experiments made on pressurized $Y_2O_3$ nanoparticles with a different defect density and published the findings elsewhere (**Figure 6a**) [6]. In the case of a highly defective sample, we observed an abrupt increase in the amorphous state contribution compared to the low-pressure crystalline phase. No high-pressure crystal is observed and the sample can be considered as amorphous, in agreement with the percolation model proposed in section 3. When a less defective sample is compressed, explosive amorphization is not observed but a competition between polymorphic transition and amorphization starts at a higher pressure than that for spontaneous amorphization. The final structure is a mixture of the high-pressure crystalline phase and the amorphous state (Figure 6b).

## 6. Conclusion

In this article, we developed different models for describing and understanding the size-dependent PIA phenomenon. The first description, the energy landscape concept, relates potential energy with atomic configurations. Interfacial effects and defects modify this energy landscape and influence the equilibrium energy and kinetics, favoring an amorphous state at some point. In a second section, we expressed the Gibbs energy, taking into account the effect of pressure on a nanoparticle but also including an interfacial energy that corresponds to the contribution of underlying and unavoidable effects related to nanomaterials, i.e., size-dependent effects such as surface state (defect, capping molecules). The effects of interfacial energies associated with elastic energy during compression correspond to energizing processes leading to amorphization of the structure. It should be noted that both approaches can also be used to describe another phenomenon more frequently encountered in nanoparticles than in bulk materials, namely polyamorphism, corresponding to a transformation from an amorphous state to a different amorphous form [7, 35].

The final two sections are dedicated to detailed descriptions of amorphization either in the case of conditions far from equilibrium (percolating model) or in the case of a competition with polymorphic transition. In both cases, the conditions required for an amorphous state of pressurized nanoparticles is as follows:

(i) An initial defect concentration must be present in the nanoparticles ($C>C_N$). Defect-free nanoparticles cannot be amorphized unless defects are generated at some point in the process. On the other hand, a defect concentration above a critical value ($C>C_c$) leads to an amorphous state under ambient conditions such as in the case of irradiation-induced amorphization. To observe a size-dependent PIA, the defect concentration should lie between $C_N$ and $C_c$.

(ii) The smaller the particles, the higher the interfacial energy becomes. Therefore, the critical defect density for amorphization becomes lower.

Size-dependent PIA is mainly driven by the defect density in the nanoparticles and their interfacial energy. These features can be controlled during sample synthesis and storage. It can be foreseen that high-pressure behavior is appropriate in order to control the quality of the nanoparticles.

**Supporting Information**
Supporting Information is available.

**Acknowledgements**
We thank Pierre Tolédano, Georges Bouzerar and Raùl Quesada for their comments and encouragements.

1 Note that only recently it has been demonstrated that no cold sintering occurred with nanoparticles (more specifically in the case of $ZrO_2$) by monitoring the vibrations of the nanoparticules under high stresses; see, for example: L. Saviot, D. Machon, A. Mermet, D.B. Murray, S. Adichtchev, J. Margueritat, F. Demoisson, M. Ariane and M.C. Marco de Lucas, Quasi-free nanoparticle vibrations in a highly compressed $ZrO_2$ nanopowder. *J. Phys. Chem. C*. 2012, **116**, 22043−22050.

2 S.H. Tolbert and A.P. Alivisatos, *Annu. Rev. Phys. Chem.* 1995, **46**, 595−626.

3 A. San Miguel, *Chem. Soc. Rev.* 2006, **35**, 876−889.

4 E. Roduner, *Chem. Soc. Rev.* 2006, **35**, 583−592.

5 A. Navrotsky, *Geochem. Trans.* 2003, **4**, 34.

6 L. Piot, S. Le Floch, T. Cornier, S. Daniele and D. Machon, *J. Phys. Chem. C* 2013, **117**, 11133−11140.

7 D. Machon, F. Meersman, M.C. Wilding, M. Wilson and P.F. McMillan, *Prog. Mater Science* 2014, **61**, 216-282.

8 A. Meldrum, L.A. Boatner and R.C. Ewing, *Phys. Rev. Lett.* 2002, **88**, 025503.

9 V. Pischedda, G.R. Hearne, A.M. Dawe and J.E. Lowther, *Phys. Rev. Lett.* 2006, **96**, 035509.

10 V. Swamy, A. Kuznetsov, L.S. Dubrovinsky, P.F. McMillan, V.B. Prakapenka, G. Shen and B.C. Muddle, *Phys. Rev. Lett.* 2006, **96**, 135702.

11 L. Wang, W. Yang, Y. Ding, Y. Ren, S. Xiao, B. Liu, S.V. Sinogeikin, Y. Meng, D.J. Gosztola, G. Shen et al. *Phys. Rev. Lett.* 2010, **105**, 095701

12 Z. Quan, Z. Luo, Y. Wang, H. Xu, C. Wang, Z. Wang and J. Fang, *Nanoletters* 2013, **13**, 3729-3735.

13 Z. Quan, Y. Wang, I.T. Bae, W. Siu Loc, C. Wang, Z. Wang and J. Fang, *Nanoletters* 2011, **11**, 5531-5536.

14 D. Machon, M. Daniel, P. Bouvier, S. Daniele, S. Le Floch, P. Mélinon and V. Pischedda, *J. Phys. Chem. C* 2011, **115**, 22286−22291.

15 D.J. Wales, *Energy Landscapes*, Cambridge university Press 2003

16 See Electronic Supplementary Information.

17 S.H. Tolbert and A.P. Alivisatos, *Science* 1994, **265**, 373−376.

18 V. Swamy, A. Kuznetsov, L.S. Dubrovinsky, R.A. Caruso, D.G. Shchukin and B.C. Muddle, *Phys Rev B* 2005, **71**, 184302.

19 D. Machon, L. Piot, D. Hapiuk, B. Masenelli, F. Demoisson, R. Piolet, M. Ariane, S. Mishra, S. Daniele, M. Hosni, N. Jouini, S. Farhat and P. Mélinon, *Nanoletters* 2014, **14**, 269 −276.

20 S. Carenco, D. Portehault, C. Boissière, N. Mézailles and C. Sanchez, *Adv. Mater.* 2014, **26**, 371-390.

21 A parallel can be drawn between this sudden transformation from crystalline to amorphous at the percolation threshold and the spontaneous crystallization of antinomy thin films (explosive crystallization) that happens at a percolation threshold corresponding to the interconnection of nanoparticles – A. Hoareau, J.X. Hu, P. Jensen, P. Mélinon, M. Treilleux and B. Cabaud, *Thin Solid Films* 1992, **209**, 161-164.

22 E.K.H. Salje, J. Chrosch and R.C. Ewing, *Am. Mineral.* 1999, **84**, 7.

23 K. Trachenko, M.T. Dove and E.K.H. Salje, *J. Appl. Phys.* 2000, **87**, 7702-7707.

24 M. Porto, S. Havlin, S. Schwarzer and A. Bunde, *Phys. Rev. Lett.* 1997, **79**, 4060.

25 When small amorphous domains appear, the fractal geometry of the high-pressure cluster (here the amorphous state) induces a power law behavior with the parameter μ given by the Hausdorff-Besicovitch space rather than the Euclidean one, and defined as $D_f = 3 - \mu$ where $D_f$ is the Hausdorff fractal dimension of the Cantor set. For a discussion of Hausdorff Besicovitch versus fractal problem see D.E. Stewart, ANZIAM J. 2001, **42**, 451.

26 Assuming that the model developed by Milovanov and Rasmussen (A.V. Milovanov and J.J. Rasmussen, *Physics Letters*, 2005, **A 337**, 75) in one dimension can be generalized to three dimensions.

27 B. Sapoval, *Universalités et fractales*, Flammarion, coll. « Champs », 2001

28 D. Stauffer and A. Aharony: *Introduction to Percolation Theory*, Revised Second Edition Taylor and Francis 1992.

29 P. Tolédano and V.P. Dmitriev, *Reconstructive Phase Transitions* (Singapore: World Scientific), 1996.

30 V.L. Ginzburg and L.D. Landau, *Sov. Phys. JETP* 1950, **20**, 1064-1082.

31 I.E. Dzialoshinskii, *Sov. Phys. JETP* 1964, **19**, 960.

32 P. Tolédano and U. Bismayer, *J.Phys.: Condens. Matter* 2005, **17**, 6627–6634.

33 P. Tolédano, *Europhys. Lett.* 2007, **78**, 46003.

34 I.A. Ovid'ko and A.G. Sheinerman, *Appl. Phys. A* 2005, **81**, 1083-1088.

35 D. Machon, M. Daniel, V. Pischedda, S. Daniele, P. Bouvier and S. LeFloch, *Phys. Rev. B* 2010, **82**, 140102.

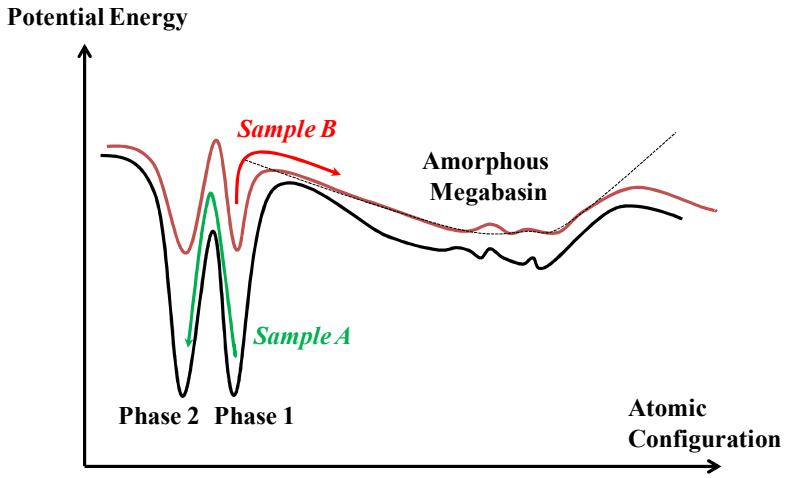


***Figure 1.*** *Energy landscapes of two nanocrystalline samples at high pressure. Sample A has a low defect density and exhibits a transition from phase 1 to phase 2. The kinetics of the transformation are controlled by the height of the energy barrier. Sample B contains a high defect density. Under pressure, transformation to the amorphous state is kinetically favorable for this sample.*

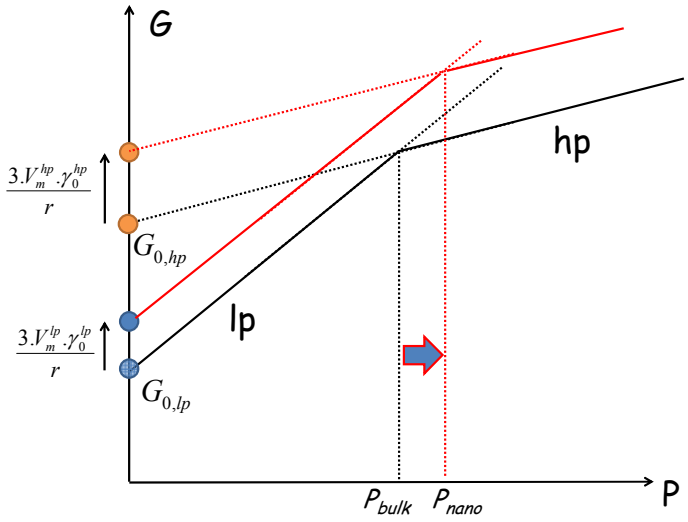


***Figure 2***. *Effect of interfacial energy on phase stability. The phase transition pressure in the bulk material is given by the crossover between the Gibbs energy function for each phase (lp for low-pressure and hp for high-pressure phases, respectively). In the case of nanoparticles, the Gibbs energy must be corrected by a surface-related term for each phase ($\gamma_0^{lp}$ and $\gamma_0^{hp}$). Usually the surface tension is higher in the high-pressure phase than in the low-pressure one, which leads to a predicted shift in the transition pressure to a higher value.*

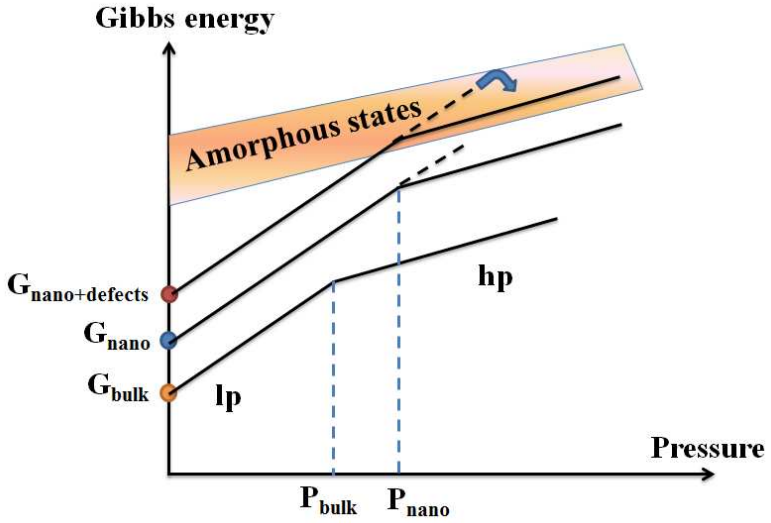


***Figure 3.*** *Gibbs energy as a function of pressure for three different morphologies of the same compound: bulk material, nanoparticles and defective nanoparticles. Interfacial energy considerations are responsible for the increase in the transition pressure (nanoparticles) or pressure-induced amorphization (defective nanoparticles).*

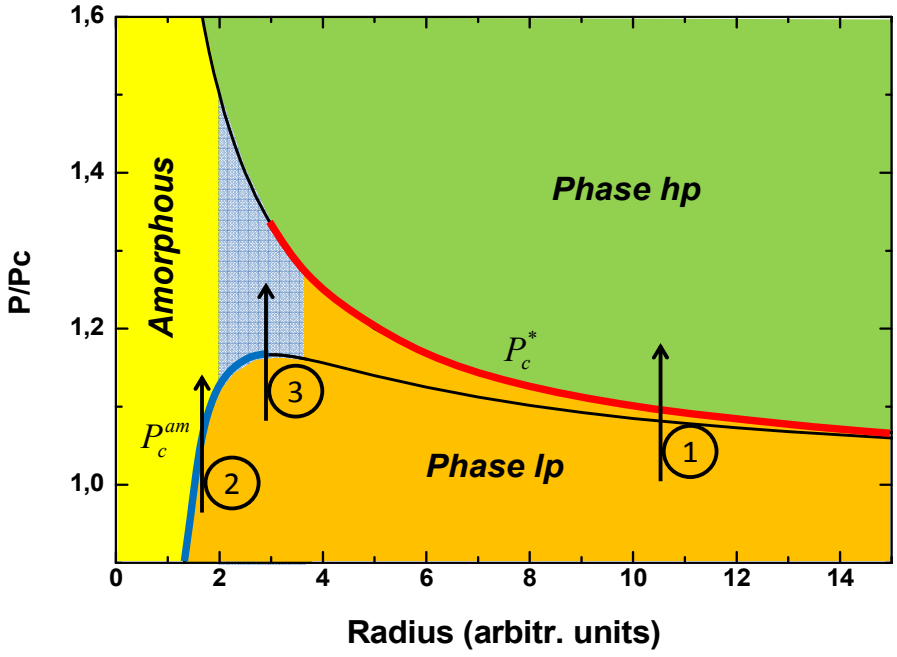


***Figure 4.*** *Schematic Phase Diagram showing different regimes. For large particles, the low-pressure phase (lp) transforms to a high-pressure phase at a higher pressure ($P_c^*$) than in the bulk material when the radius decreases (red line). Once a critical size (depending on the material, the surface state and the defect density) is reached, there exists a cross-over between this polymorphic transition and pressure-induced amorphization ($P_c^{am}$). In this case, the amorphization pressure decreases with decreasing size (blue line).*

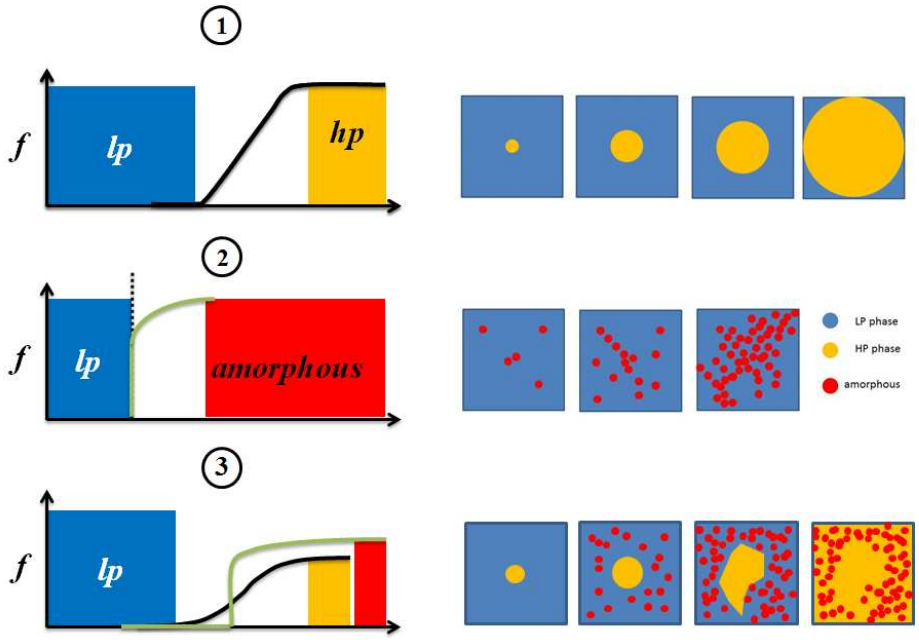


***Figure 5***. *Summary of the different scenarios during the pressurization of nanoparticles. In case 1, far from the critical region (see figure 4), the defect concentration is not sufficient to induce amorphization. In this case, transformation occurs in the form of a cooperative, homogeneous movement of many atoms that result in a change in the crystal structure. The growth of the high-pressure phase within the low-pressure phase is homogeneous and is well-described in Euclidean space. In case 2, the defect density is sufficient to induce a percolating system of amorphous domains. Case 3 is the situation where two competing processes exist: polymorphic and amorphization transition. The final state is coexisting amorphous and high-pressure crystalline phases.*

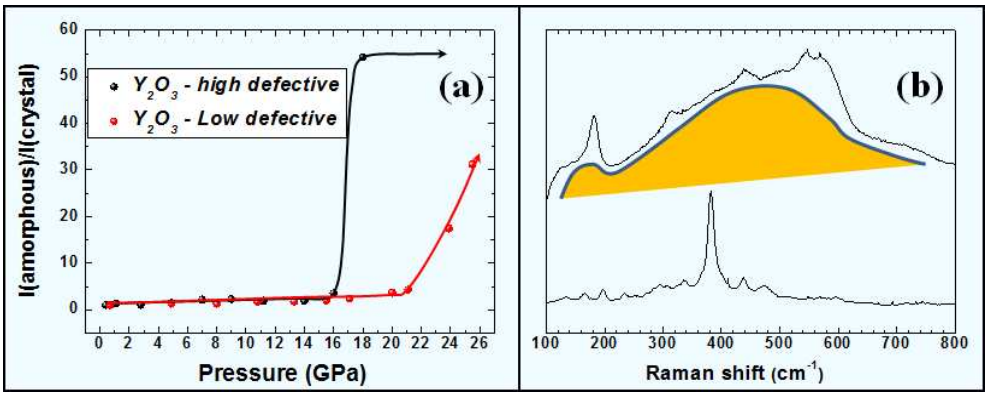


***Figure 6.*** *a) ratio of the amorphous and crystalline (low-pressure phase) contributions to Raman spectra of $Y_2O_3$ nanoparticles under pressure. Two types of sampled are considered: i) highly-defective nanoparticles (black). In this case, explosive amorphization is observed as the percolating threshold is reached; ii) less defective nanoparticles (red). The number of sites transforming to an amorphous state is below the percolating threshold. The ratio increases as the low-pressure phase transforms to the high-pressure structure. b) in the final state amorphous and high-pressure crystalline phases coexist, as observed by Raman spectroscopy (broad orange peak: amorphous state).*